

Singularities of a Manipulator with Offset Wrist

Robert L. Williams II

Department of Mechanical Engineering
Ohio University
Athens, Ohio

Journal of Mechanical Design

Vol. 121, No. 2, pp. 315-319
June, 1999

AUTHOR INFORMATION:

Robert L. Williams II
Department of Mechanical Engineering
257 Stocker Center
Ohio University
Athens, OH 45701-2979
phone: (740) 593-1096
fax: (740) 593-0476
email: bobw@bobcat.ent.ohiou.edu

SINGULARITIES OF A MANIPULATOR WITH OFFSET WRIST

Robert L. Williams II

Department of Mechanical Engineering
Ohio University
Athens, Ohio

ABSTRACT

The singularities of manipulators with offset wrists are difficult to enumerate. This article presents a numerical study to illuminate singularity problems when using an offset wrist with an articulated regional arm. Ironically, the regional manipulator singularity problem is worsened when using a singularity-free offset wrist. No wrist singularities exist (they are forced by design to lie outside of joint limits). However, the existing regional arm singularities become skewed from the well-known singular configurations of common manipulators. The wrist offset also skews the well-known wrist singularities (though they hopefully still lie outside of joint limits, their locations are no longer easily determined). Thus, a zero-offset singularity-free wrist is preferable with regard to overall manipulator singularities.

INTRODUCTION

Manipulator singularities can be found from the manipulator Jacobian matrix J : $|J| = 0$ for non-redundant manipulators and $|JJ^T| = 0$ for kinematically-redundant manipulators. The linearized rate relationship is expressed $\{v \ \omega\}^T = [J]\{\dot{\Theta}\}$, where v are the translational Cartesian velocities, ω are the rotational Cartesian velocities, and $\{\dot{\Theta}\}$ are the joint rates. For a manipulator with a spherical (zero-offset) wrist, the upper right Jacobian submatrix is the 3x3 zero matrix, which is the velocity-domain manifestation of position/orientation decoupling. Singularities are classified as regional arm

singularities (found from $|J_{UL}| = 0$) and wrist singularities (found from $|J_{LR}| = 0$) (Stanisic and Duta, 1990).

$$[J] = \begin{bmatrix} [J_{UL}] & [0] \\ [J_{LL}] & [J_{LR}] \end{bmatrix}; \quad |J| = |J_{UL}| |J_{LR}| \quad (1)$$

For a manipulator with an offset wrist the Jacobian matrix $[\bar{J}]$ is fully populated as in Eq. 2. This is because some wrist joints participate in translation of the last wrist frame in addition to orientation. In this case, the singularities can no longer be classified as separate regional arm singularities and wrist singularities (Stanisic and Duta, 1990).

$$[\bar{J}] = \begin{bmatrix} [\bar{J}_{UL}] & [\bar{J}_{UR}] \\ [\bar{J}_{LL}] & [\bar{J}_{LR}] \end{bmatrix}; \quad |\bar{J}| \neq |\bar{J}_{UL}| |\bar{J}_{LR}| \quad (2)$$

Singularity-free, offset double universal joint (DUJ) wrists (Fig. 1) have been designed and built by Trevelyan, et. al. (1986), Milenkovic (1987), and Rosheim (1987). The Jacobian matrix determinant for the DUJ wrist alone is $|J_{DUJ}| = 4c_5c_6^2$ ($c_i = \cos \theta_i$) so the singularity conditions are $\theta_5 = \pm 90$ (all angles in this article are given in degrees) or $\theta_6 = \pm 90$. If these are forced to lie outside of joint limits, the wrist is singularity-free (Williams, 1990).

In this paper, the 3-axis DUJ wrist is mounted on an articulated 3-axis regional arm (Fig. 2; PUMA with no waist-shoulder offset, i.e. $L_0=0$) to form a 6-dof manipulator. There are eight rows in the DH parameters (Table I, Craig (1989) convention) because the DUJ wrist mechanically couples the two universal joints (which are separated by offset L). This mechanical coupling is usually accomplished via two gear pairs, shown conceptually in Fig. 1. The joint angle offsets in Table I are included to define the zero position as straight up.

The regional arm singularities for the first three joints alone are found symbolically from

$$|J_{reg}| = L_1 L_2 (L_1 s_2 + L_2 s_{23}) s_3 = 0, \quad \text{where } s_i = \sin \theta_i \quad \text{and} \quad s_{23} = \sin(\theta_2 + \theta_3). \quad \text{The non-trivial}$$

singularity conditions are $L_1s_2 + L_2s_{23} = 0$ (when the wrist point lies on the plane through the waist and shoulder axes, there is no side-to-side translation possible) and $\theta_3 = 0,180$ (elbow straight or folded workspace boundary singularity).

It follows from Eq. 2 that the four regional arm and wrist singularity conditions ($L_1s_2 + L_2s_{23} = 0$, $\theta_3 = 0,180$, $\theta_5 = \pm 90$, $\theta_6 = \pm 90$) do not necessarily exist for the articulated arm with offset DUJ wrist. In fact, only $\theta_6 = \pm 90$ remains as a singularity because c_6 is a multiple in the symbolic determinant. However, from Eq. 1, these same four conditions are the complete singularity enumeration if $L=0$. As L increases from 0, what happens to these singular conditions?

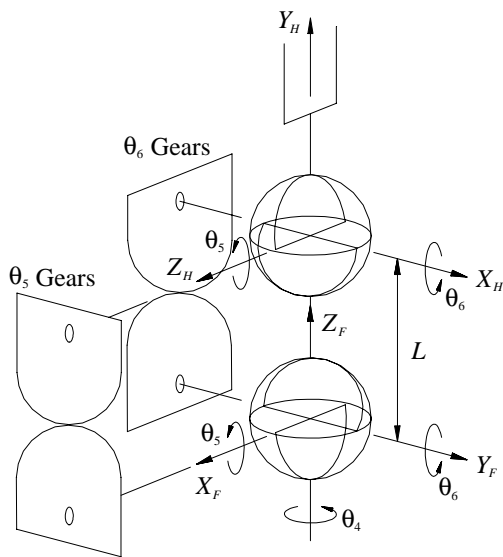


Figure 1
Double-Universal Joint (DUJ) Wrist

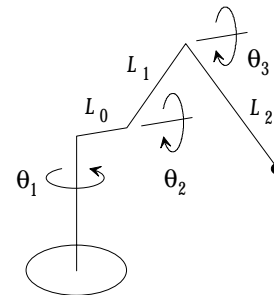


Figure 2
Regional Arm

Table I. Articulated Arm with DUJ Wrist DH Parameters

i	α_{i-1}	a_{i-1}	d_i	θ_i
1	0	0	0	θ_1
2	-90	0	$L_0=0$	$\theta_2 - 90$
3	0	L_1	0	$\theta_3 + 90$
4	90	0	L_2	θ_4
5	90	0	0	$\theta_5 + 90$
6	90	0	0	θ_6
7	0	L	0	θ_6
8	-90	0	0	$\theta_5 - 90$

MANIPULATOR SINGULARITY DETERMINATION

Many authors have presented results in manipulator singularity analysis (e.g. Kholi and Hsu, 1987, and Waldron et.al., 1985). In a singular configuration, a singular screw exists which is simultaneously reciprocal to all n joint axis screws (Sugimoto et.al., 1982). In a significant work, Burdick (1995) exploits this theorem to develop two analogous recursive algorithms to determine the complete singularity set for generic and non-generic revolute-jointed manipulators (most industrial manipulators are non-generic, which encounter bifurcations). The two algorithms, one for regional singularities and the other for twist singularities, may be used symbolically or numerically, but complexity grows rapidly in the symbolic case. The Jacobian does not need to be determined, and the singular screw is calculated in each case.

Burdick's algorithms were applied numerically to the present non-generic manipulator with offset DUJ wrist. However, the results are difficult to interpret for the purpose of singularity enumeration. Burdick's algorithms trace singular surfaces (in joint space, mapped to the Cartesian space). This is done on workspace cross-section planes, which is good to show the extent of the problem, but orientation information is lost. Therefore, to demonstrate (in joint space) what happens to the singular conditions as L increases from 0, numerical searches of the Jacobian matrix determinant were performed.

The determinant of the Jacobian matrix (given the DH parameters of Table I) was determined symbolically. The simplest symbolic terms result when the frame of expression is in the middle of the manipulator (in this case, the elbow frame, whose origin is the intersection of L_1 and L_2 , whose Z axis is the rotation axis for θ_3 , and whose X axis lies along L_2 in Fig. 2). Note the Jacobian still gives Cartesian velocities of the last moving frame with respect to the base, but the basis for expression is the elbow frame. The determinant is invariant under coordinate transformations. Due to the mechanical wrist coupling, Table I rows 5 and 8 both involve θ_5 and rows 6 and 7 involve θ_6 .

Columns 5 and 8 of the symbolic Jacobian multiply $\dot{\theta}_5$ while columns 6 and 7 multiply $\dot{\theta}_6$. Therefore, the 6x6 Jacobian is formed by adding columns 5 and 8 for the fifth column and adding columns 6 and 7 for the sixth column. The Jacobian determination algorithm used recognizes each i^{th} column of the Jacobian as the Cartesian velocity of the last moving frame due to joint i alone (with $\dot{\theta}_i$ factored out).

$$|\bar{J}| = L_1 c_6 [\{ (2c_6(2k_4 k_5 + k_1) + k_3) s_4 s_6 + 2 \{ (-k_1 c_4 s_5 + k_2 c_5^2 + (1 - 2c_4^2) k_4) c_6^2 + k_2 \} \} L + \{ (4L_2^2 + L^2) s_{23} + 4L_1 L_2 s_2 \} s_3 c_5 - L k_3 k_5 \} c_6] \quad (3)$$

where $k_1 = (L_1 s_2 + L_2 s_{23}) c_3 c_5$, $k_2 = (L_1 s_2 c_4^2 + L_2 s_{23}) s_3$, $k_3 = L s_{23} c_3$, $k_4 = L_1 s_2 s_3$, $k_5 = c_4 s_5$.

If $L=0$ is substituted into Eq. 3, the result is: $|J| = |J_{UL}| |J_{LR}| = L_1 L_2 (L_1 s_2 + L_2 s_{23}) s_3 c_5 c_6^2$, from which the four zero-offset singularities are evident.

RESULTS

To investigate the effect of L on manipulator singularities, multi-dimensional computer numerical searches were performed on the symbolic determinant expression, Eq. 3. Singularities are independent of θ_1 . For comparison purposes, $L_1 = 0.9m$ and $L_2 = 1.1m$ (chosen for generality and reasonable scaling between translational and rotational Jacobian components). The reciprocal condition number may be a better measure of absolute Jacobian matrix conditioning, but since the purpose was to compare two manipulators identical except for wrist offset L , the Jacobian determinant, Eq. 3, was sufficient. To present graphical results, a series of 2-axis searches was performed (varying all possible combinations of θ_i, θ_j ($i, j = 2, 3, \dots, 6; i \neq j$)) while the remaining joint angles were fixed. The fixed angles were set both far from the zero-offset singularities ($\Theta_{2-6} = \{20 \ 60 \ 40 \ 10 \ 15\}$) and near ($\Theta_{2-6} = \{20 \ 5 \ 40 \ 85 \ 85\}$), with similar results (except for the magnitude of the Jacobian determinant!). Only the former case results are shown below, where three of the angles are fixed and two vary. θ_i, θ_j were varied over ± 180 in steps $\Delta\theta = 1$.

A typical determinant surface plot is shown in Fig. 3 for $i=3, j=5$, and $L=0$.

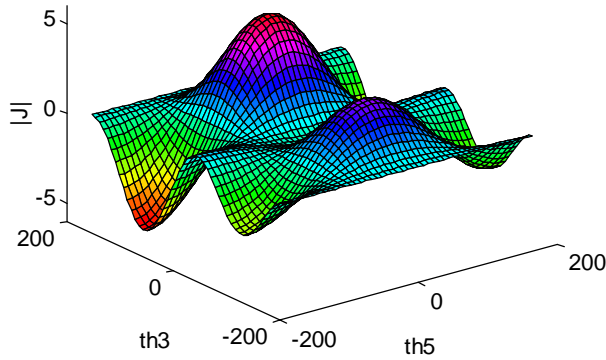


Figure 3. θ_3, θ_5 Determinant Surface Plot, $L=0$

For $L=0$, the singularity conditions $\theta_3 = 0, 180$, $\theta_5 = \pm 90$, and $L_1 s_2 + L_2 s_{23} = 0$ ($\theta_{3 \sin g} = -36.2$ given the fixed $\theta_2 = 20$) appear in the left contour plot of Fig. 4. The right contour plot of Fig. 4 is for the same case, with $L=0.3$. The $L=0$ singularity conditions are recognizable, but their locations are skewed.

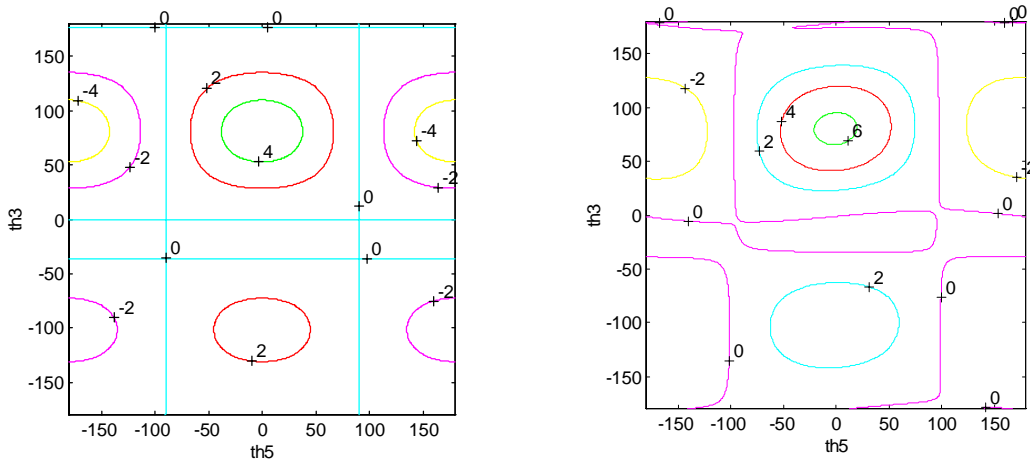


Figure 4. θ_3, θ_5 Determinant Contour Plot

Figure 5 shows $i=2, j=3, L=0$ (solid lines) and $L = 0.4$, (dashed lines). This and all remaining figures show only the zero contour lines, comparing $L=0$ and $L \neq 0$. $L=0$ singularity conditions $\theta_3 = 0, 180$ and $L_1 s_2 + L_2 s_{23} = 0$ (multiple solutions) appear as solid lines. Figures 6 shows the effect increasing L has on this case. Here $i=2, j=3, L=0$ (solid lines) and $L = 0.1, 0.2, 0.3, 0.4$, (dashed lines, top left, top right, bottom left, and bottom right, respectively). One quarter of the Fig. 5 range is shown, for clarity.

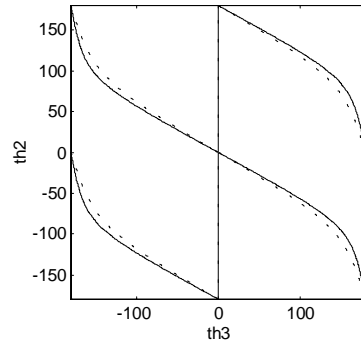


Figure 5. θ_2, θ_3 Determinant Zero-Contour Plot

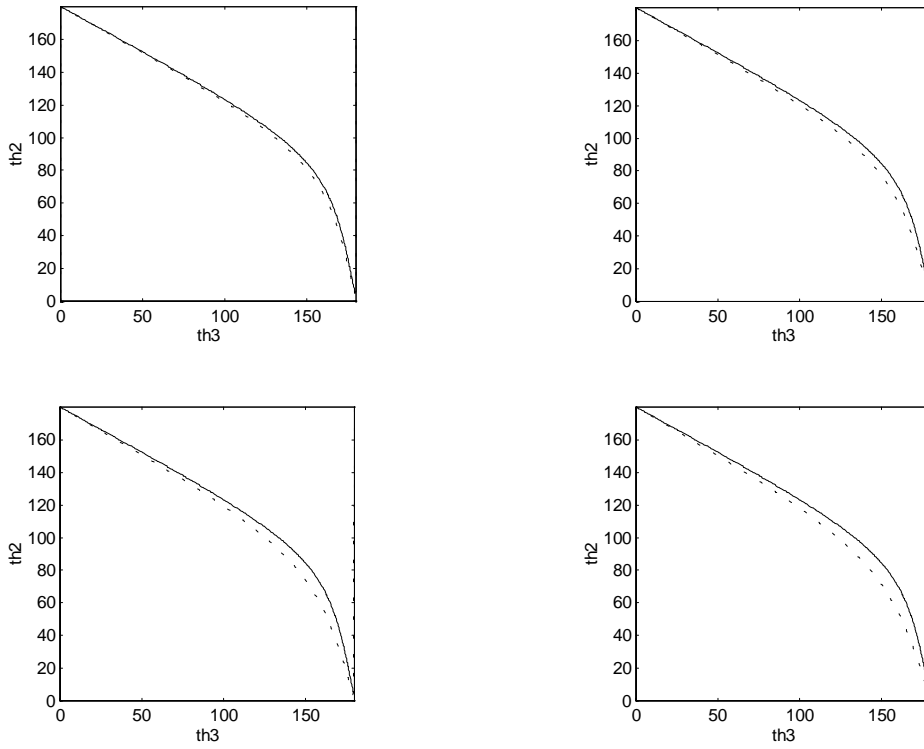


Figure 6. θ_2, θ_3 Zero Determinant, Increasing L

A subset of the remaining 2-axis search plots are given below, comparing $L=0$ (solid lines) and $L = 0.3$ (dashed lines). θ_4 does not affect the $L=0$ determinants and it weakly affects the $L \neq 0$ determinants.

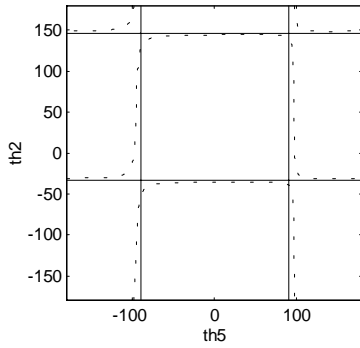


Figure 7. θ_2, θ_5 Zero Determinant

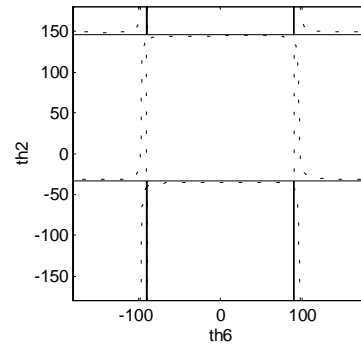


Figure 8. θ_2, θ_6 Zero Determinant

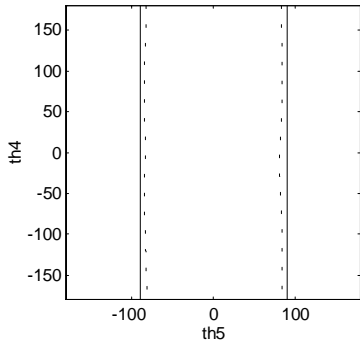


Figure 9. θ_4, θ_5 Zero Determinant

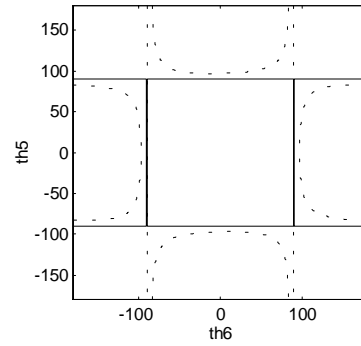


Figure 10. θ_5, θ_6 Zero Determinant

In Figs. 8 and 10, the $\theta_6 = \pm 90$ singularity lines are shared by the $L=0$ and $L \neq 0$ cases.

For a more complete singularity analysis (albeit difficult to present graphically), nested 5-axis searches were also performed (ignoring θ_1). Different L values were specified; for each, average and maximum Jacobian determinant absolute values were recorded (O and X on Fig. 11 left, respectively), in addition to the percentage of cases where $abs(\overline{J}) \leq \varepsilon = 0.01$ (Fig. 11 right). θ_i ($i = 2, 3, \dots, 6$) were varied over ± 45 in steps $\Delta\theta = 1$.

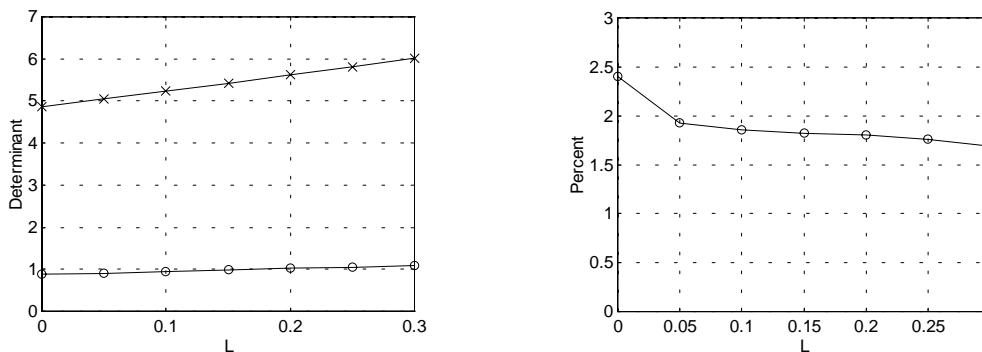


Figure 11. 5-Axis Determinant Search Dexterity Measures

The purpose of the simulation data presented in Fig. 11 is to study the average overall manipulator dexterity as the wrist offset L increases. As seen by the maximum and average determinants increasing as L increases and the percentage of near-zero determinants decreasing as L increases, the manipulator dexterity improves as L increases. However, the difference is not dramatic, and the overall manipulator singularity behavior is less predictable as L increases (see Fig. 6).

CONCLUSION

Knowledge of manipulator singularity conditions is important for task design, path planning, and manipulator control. The singularity conditions for a manipulator with an offset wrist exist in the same neighborhoods as those for the same manipulator with zero-offset wrist, but their locations are skewed. As the offset L grows, the skewing is more pronounced. With non-zero offset L , the singular conditions are difficult to enumerate because they can no longer be classified using position/orientation decoupling $|J| = |J_{UL}||J_{LR}|$. For the two-joint-angle searches, analytical expressions could be derived for the $L \neq 0$ singularities, but this would be of little value because the remaining joint angles are fixed arbitrarily. The full five-joint-angle $L \neq 0$ singularity conditions (independent of θ_1) have not been derived due to symbolic complexity.

As L increases, most known $L=0$ singular conditions are no longer exact singularities. Also, manipulator dexterity improves slightly (measured by Jacobian matrix determinant average and maximum and the percentage of cases where $abs(\overline{|J|}) \leq \epsilon = 0.01$) as L increases. However, as L increases, the wrist subassembly also becomes less wrist-like and significant translations of the last wrist frame are caused by some wrist joints.

Therefore, the irony is that with singularity-free offset DUJ wrists, the regional manipulator singularity problem is actually worsened. There are no wrist singularities (because they are placed by design outside of joint limits), but the existing regional arm singularities become skewed from the well-known singular configurations of common industrial designs. More recently, other researchers (Lee et.al, 1996; Stanasic and Duta, 1990) have developed zero-offset singularity-free wrists. Based on manipulator kinematics and the overall manipulator singularity problem, the zero-offset wrist is preferable.

REFERENCES

Burdick J.W., 1995, "A Recursive Method for Finding Revolute-Jointed Manipulator Singularities", *Journal of Mechanical Design*, Vol 117, pp. 55-63.

J.J. Craig, 1989, *Introduction to Robotics: Mechanics and Control*, Addison Wesley Publishing Co., Reading, MA.

Kholi D. and Hsu M.S., 1987, "Boundary Surfaces and Accessibility Regions for Regional Structures of Manipulators", *Mechanism and Machine Theory*, Vol 22, No. 3, pp. 277-289.

Lee K.M., Roth R.B. and Zhou Z., 1996, "Dynamic Modeling and Control of a Ball-joint-Like Variable Reluctance Spherical Motor", *Journal of Dynamic Systems, Measurement, and Control*, Vol 118, No. 1, pp. 29-40.

Milenkovic, V., 1987, "New Nonsingular Robot Wrist Design", *Robots 11 Conference Proceedings RI/SME*, Chicago, IL, pp. 13.29-13.42.

Rosheim, M.E., 1987, "Singularity-Free Hollow Spray Painting Wrists", *Robots 11 Conference Proceedings RI/SME*, Chicago, IL, pp. 13.7-13.28.

Stanisic, M.M., and Duta, O., 1990, "Symmetrically Actuated Double Pointing Systems: The Basis of Singularity-Free Robot Wrists", *IEEE Transactions on Robotics and Automation*, Vol. 6, No. 5.

Sugimoto K., Duffy J. and Hunt K.H., 1982, "Special Configurations of Spatial Mechanisms and Robot Arms", *Mechanism and Machine Theory*, Vol 17, No. 2, pp. 119-132.

Trevelyan, J.P., Kovesi, P.D., Ong, M., and Elford, D., 1986, "ET: A Wrist Mechanism Without Singular Positions", *The International Journal of Robotics Research*, Vol. 4, No. 4, pp. 71-85.

Waldron K.J., Wang S.L. and Bolin S.J., 1985, "A Study of the Jacobian Matrix of Serial Manipulators", *Journal of Mechanisms, Transmissions, and Automation in Design*, Vol 107, pp. 230-238.

Williams R.L. II, 1990, "Forward and Inverse Kinematics of Double Universal Joint Robot Wrists", *Proceedings of the 1990 Space Operations, Applications, and Research (SOAR) Symposium*, Albuquerque, NM.